Electrically Driven Reverse Overhauser Pumping of Nuclear Spins in Quantum Dots

M. S. Rudner and L. S. Levitov

Department of Physics, Massachusetts Institute of Technology, 77 Massachusetts Avenue, Cambridge, Massachusetts 02139, USA

(Received 4 October 2007; published 13 December 2007)

We propose a new mechanism for polarizing nuclear spins in quantum dots, based on periodic modulation of the hyperfine coupling by electric driving at the electron spin resonance frequency. Dynamical nuclear polarization results from resonant excitation rather than hyperfine relaxation mediated by a thermal bath, and thus is not subject to Overhauser-like detailed balance constraints. This allows polarization in the direction opposite to that expected from the Overhauser effect. Competition of the electrically driven and bath-assisted mechanisms can give rise to spatial modulation and sign reversal of polarization on a scale smaller than the electron confinement radius in the dot.

DOI: 10.1103/PhysRevLett.99.246602 PACS numbers: 72.25.Pn, 05.65.+b, 05.70.Ln, 72.25.Rb

Advances in semiconductor quantum dot technology have given experimentalists unprecedented control over electron and nuclear spins, leading the way to many exciting applications in spintronics and quantum information processing. Coherent control of electron spins has been demonstrated in few-electron double quantum dots [1–3]. Because electron spin decoherence in GaAs quantum dots arises mainly due to coupling to the disordered nuclear spin system [4,5], there is great interest in developing new ways of controlling nuclear spins [6,7].

Nuclear spin polarization has been achieved in double dots in the spin-blockaded dc transport regime where the hyperfine interaction couples the electron and nuclear spins [8–10]. Also, recent experiments on electron spin resonance (ESR) in quantum dots [2,3] have demonstrated dynamical nuclear polarization (DNP) through resonant driving of ESR by electric and magnetic fields. Interestingly, DNP was found [3,11] to be in the direction opposite to that expected from the thermodynamic arguments [12,13] that explain the direction of pumping in previous experiments [14,15]. Thus a new mechanism of nuclear spin pumping must be found.

The essence of the Overhauser pumping mechanism [12,13] is that a large mismatch of Zeeman energies prevents mutual electron-nuclear spin flips without coupling to an external bath, e.g., phonons. Pumping occurs in the direction determined by the constraint that at low temperatures the bath can only accept energy from the system: spin flips occur primarily via spontaneous emission of excitations into the bath [see Fig. 1(a)].

In Refs. [2,3], DNP is observed as an ESR frequency shift due to the longitudinal part of the hyperfine interaction between the electron spin $\hat{S}$ and all nuclear spins $\{\hat{I}_k\}$, $\hat{H}^{\mathrm{HF}} = A\sum_k |\psi(\mathbf{r}_k)|^2 \hat{\mathbf{S}} \cdot \hat{\mathbf{I}}_k$, where A is the hyperfine constant, $\psi(\mathbf{r})$ is the electron envelope wave function, and $\{\mathbf{r}_k\}$ are the positions of the nuclei. Because of this shift, the electron Zeeman energy becomes

$$\Delta\varepsilon = |g\mu B_0 - An_0 s|, \tag{1}$$

where n_0 and $s \sim \sum_k \langle \hat{I}_k^z \rangle$ are the density and effective polarization of nuclei [see Eq. (4)].

The sign of the frequency shift is determined by the direction of polarization and by the relative signs of A, μ, and the electron g factor. In GaAs, $An_0 \approx 130\ \mu$eV and $g \approx -0.4$. Because the electron spin points up in the ground state, the thermodynamic argument [12,13] predicts a negative polarization $s < 0$ and hence a positive

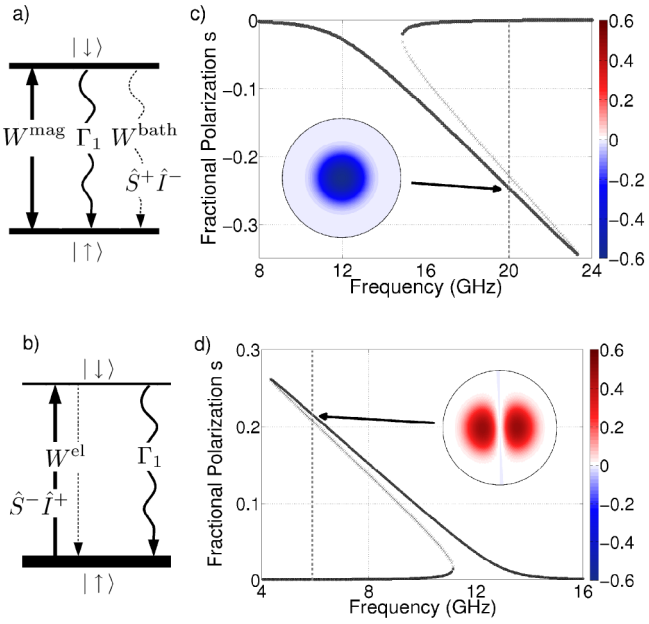

FIG. 1 (color online). Nuclear polarization in (a),(c) the Overhauser and (b),(d) the reverse Overhauser regimes. Panels (a) and (b) display the key transitions between electron Zeeman levels due to magnetic/electric ESR driving, $W^{\mathrm{mag,el}}$, bath-assisted hyperfine relaxation, and electron spin relaxation, $W^{\mathrm{bath}} \ll \Gamma_1$. Dominant electron-nuclear spin-flip processes are marked by $\hat{S}^{\pm}\hat{I}^{\mp}$. Panels (c) and (d) show the steady-state nuclear polarization determined self-consistently via Eq. (4) combined with (9) and (10). Insets show the spatial distribution of nuclear polarization in a circular region of radius 50 nm, obtained using the electron density $|\psi(r)|^2 \propto e^{-r^2/r_0^2}$ with $r_0 = 25$ nm.

frequency shift, in contrast to the observed shift toward *lower* frequency [3,11].

However, in the situation [3] where hyperfine flip-flop transitions are stimulated by an externally applied time-varying electric field, the direction of pumping is not set by the relaxational energy balance of hyperfine transitions. Rather, pumping occurs when nonhyperfine mechanisms of electron spin relaxation replenish the population of the electron spin ground state [see Fig. 1(b)], thus allowing many nuclear spins to be pumped in the direction selected by electron spin *excitation*.

To compare this effect with the usual Overhauser mechanism, it is instructive to extend the model to include magnetic driving and bath-assisted hyperfine relaxation. By solving a self-consistency equation for the effective nuclear polarization s, we map out the fixed points of DNP (see Fig. 1). We find spatial modulation on a scale less than the electron confinement radius, and complex, history-dependent ESR shifts in the crossover regime where the two mechanisms act in direct competition.

We note that an Overhauser-like mechanism involving spin flips caused by nonsecular terms of the dipole-dipole interaction such as $\hat{S}^+\hat{I}_k^+$ [13] can lead to ''inverted'' DNP [16]. However, because the electron-nuclear dipole coupling is weak in GaAs this mechanism cannot explain the results of experiments [2,3].

The driving of ESR by coupling a localized electron to an electric field $\mathbf{E}(t) \propto \mathbf{E}_\omega e^{-i\omega t}$ in the presence of an inhomogeneous nuclear spin distribution is described, in the harmonic approximation [3], by the Hamiltonian

$$\hat{H}^{\mathrm{el}}(t) = \frac{A}{2}\sum_k \mathbf{d}_\omega \cdot \nabla |\psi(\mathbf{r}_k)|^2 (\hat{S}^+\hat{I}_k^- e^{-i\omega t} + \mathrm{H.c.}), \quad (2)$$

where $\mathbf{d}_\omega \propto \mathbf{E}_\omega$ is the electron displacement due to the ac field [3]. Because the hyperfine interaction conserves spin, electron spin flips caused by (2) are accompanied by compensating nuclear spin flips in the opposite direction.

We assume that the electron decoheres quickly enough to prevent the entanglement of electron and nuclear spins so that we can describe the system by the factorized density matrix $\hat{\rho} = \hat{\rho}_{\mathrm{el}} \otimes \hat{\rho}_{\mathrm{N}}$. The time for this entanglement to build up was analyzed in Ref. [17] and found to be $T_{\mathrm{ent}} \approx N\Delta\varepsilon/(An_0)^2$, where N is the number of nuclear spins. If the electron decoherence rate $\Gamma_2 > 1/T_{\mathrm{ent}}$, then this entanglement is inessential for our analysis. Furthermore, we assume that the electron spin decoheres much faster than the rate of spin flips induced by (2), allowing this process to be treated as incoherent. In this limit, described by $\hat{\rho}_{\mathrm{el}} = n_+|\uparrow\rangle\langle\uparrow| + n_-|\downarrow\rangle\langle\downarrow|$, the transition rate can be calculated using Fermi's golden rule.

In this incoherent regime it is straightforward to understand the pumping mechanism and its direction. Additionally, this approach may help to understand experiments [3] where coherent Rabi oscillations were not observed. While coherence in some systems (e.g., [2]) may be higher than assumed in our model, we do not expect that it can reverse the direction of polarization.

For simplicity we consider the case of spin-1/2 nuclei and calculate the spin-flip rates for each nucleus independently using a nuclear state of the form

$$\hat{\rho}_{\mathrm{N}} = \bigotimes_k (N_{k,+}|\uparrow\rangle\langle\uparrow| + N_{k,-}|\downarrow\rangle\langle\downarrow|).$$

Here $N_{k,\pm}$ is the occupation probability of the up (down) spin state of nucleus k, with $N_{k,+} + N_{k,-} = 1$.

After a straightforward calculation, we find the spin-flip transition rate W_k^{el} for the nucleus at position $\mathbf{r}_k$

$$W_k^{\mathrm{el}} = \frac{A^2}{4}(\mathbf{d}_\omega \cdot \nabla |\psi(\mathbf{r}_k)|^2)^2 \frac{\Gamma_2}{(\omega - \Delta\varepsilon)^2 + (\Gamma_2/2)^2}, \quad (3)$$

where $\Delta\varepsilon$ is the electron Zeeman energy (1), measured in units of frequency. Parenthetically, because the electrical excitation involves simultaneous electron and nuclear spin flips, the energy $\Delta\varepsilon$ should include the nuclear Zeeman energy which is small and will be ignored hereafter. The effective fractional polarization of nuclei contributing to the Overhauser shift is

$$s \equiv \sum_k |\psi(\mathbf{r}_k)|^2 \delta V (N_{k,+} - N_{k,-}), \quad (4)$$

where δV is the unit cell volume, $\delta V = n_0^{-1}$.

The net spin-flip rate for nucleus k is determined by the upward and downward flip rates due to electric driving with rate W_k^{el} and out diffusion with rate γ:

$$\dot{N}_{k,+} = W_k^{\mathrm{el}}(n_+ N_{k,-} - n_- N_{k,+}) + \gamma(N_{k,-} - N_{k,+}). \quad (5)$$

Similarly, the electron state evolves according to

$$\dot{n}_+ = \sum_k W_k^{\mathrm{el}}(n_- N_{k,+} - n_+ N_{k,-}) + \Gamma_1 n_- - \tilde{\Gamma}_1 n_+. \quad (6)$$

The electron spin-flip rate includes contributions from all nuclei. Relaxation responsible for the rate Γ_1 can be of any origin that does not involve coupling to nuclear spins; a likely candidate is cotunneling to the leads with spin exchange. The forward and reverse relaxation rates are related by a Boltzmann factor $\tilde{\Gamma}_1 = e^{-\beta\Delta\varepsilon}\Gamma_1$ in accordance with detailed balance. The incoherent driving model (5) and (6) is valid when $\Gamma_2 \gg W^{\mathrm{el}} \equiv \sum_k W_k^{\mathrm{el}}$.

The resulting polarization is determined by the steady states of the combined system (5) and (6). The sign of polarization can be exhibited immediately by summing Eq. (5) over all k and combining it with Eq. (6):

$$\sum_k (N_{k,+} - N_{k,-}) = \frac{\Gamma_1}{\gamma}(n_- - e^{-\beta\Delta\varepsilon} n_+). \quad (7)$$

ESR driving upsets the electron equilibrium, which makes $n_- \geq e^{-\beta\Delta\varepsilon} n_+$ and leads to positive (reverse Overhauser) polarization (7). Even at weak driving when $n_- \approx e^{-\beta\Delta\varepsilon} n_+$, the polarization can still be large if nuclear relaxation is sufficiently slow: $\gamma \ll \Gamma_1$.

To compare our mechanism with the Overhauser pumping mechanism, and to facilitate the discussion of steady states, it is useful to introduce driving due to a transverse ac

magnetic field of strength B_1

$$W^{\mathrm{mag}} = \frac{1}{4}\frac{(g\mu_B B_1)^2\Gamma_2}{(\omega - \Delta\varepsilon)^2 + (\Gamma_2/2)^2}, \tag{8}$$

which adds an additional term $W^{\mathrm{mag}}(n_- - n_+)$ to (6). As in the case of electric driving, we assume $W^{\mathrm{mag}} \ll \Gamma_2$.

In principle, Γ_1 and Γ_2 can differ by many orders of magnitude. When $\Gamma_1 \ll \Gamma_2$, our rate equation approach can treat both the weak driving $W^{\mathrm{mag,el}} \ll \Gamma_1$ and strong driving $\Gamma_1 < W^{\mathrm{mag,el}} \ll \Gamma_2$ limits. If $\Gamma_1 \sim \Gamma_2$, however, the rate equation approach is valid in the weak driving limit. To treat strong driving in this regime, one must solve the full Bloch equations for electron spin [18].

The Overhauser mechanism relies on bath-assisted hyperfine relaxation. This rate includes a product of two factors describing the coupling to the bath and the hyperfine interaction, giving spatial dependence $W_k^{\mathrm{bath}} \propto |\psi(r_k)|^4$. We account for this process by adding the term $W_k^{\mathrm{bath}}(N_{k,-}n_+ - e^{-\beta\Delta\varepsilon}N_{k,+}n_-)$ to (5). Because $\sum_k W_k^{\mathrm{bath}} \ll \Gamma_1$, we neglect its contribution to Eq. (6).

The local steady state of nuclear spins is described by

$$\frac{N_{k,+}}{N_{k,-}} = \frac{(W_k^{\mathrm{el}} + \tilde{W}_k^{\mathrm{bath}})n_+ + \gamma}{(W_k^{\mathrm{el}} + W_k^{\mathrm{bath}})n_- + \gamma}. \tag{9}$$

The competition between the Overhauser and reverse Overhauser mechanisms exhibited by Eq. (9) is simplest to understand in the absence of nuclear spin relaxation, $\gamma = 0$. When electric driving is weak compared with bath-assisted relaxation, $W_k^{\mathrm{el}} < W_k^{\mathrm{bath}}$, saturating ESR by W^{mag} makes $n_+ \approx n_-$ and causes the nuclei to polarize opposite to the external field: $N_{k,+}/N_{k,-} \approx \exp(-\Delta\varepsilon/k_BT) < 1$. However, if W_k^{bath} is small compared with W_k^{el}, then Eq. (9) simplifies to $N_{k,+}/N_{k,-} \approx n_+/n_-$. Because of electron relaxation, $n_+/n_- > 1$ and nuclei polarize in the reverse Overhauser direction.

To describe this competition quantitatively, we consider a simple limit $W^{\mathrm{mag}} \gg W^{\mathrm{el}}$ where

$$\frac{n_+}{n_-} \approx \frac{W^{\mathrm{mag}} + \Gamma_1}{W^{\mathrm{mag}} + \tilde{\Gamma}_1}. \tag{10}$$

Although electric driving has a negligible effect on the electron state in this limit, it still dominates the nuclear dynamics when $W_k^{\mathrm{bath}} < W_k^{\mathrm{el}}$. If electric driving is not weak, the rates $\sum_k W_k^{\mathrm{el}} N_{k,\pm}$ appear in the numerator and in the denominator of Eq. (10). This complicates the mathematics without changing the results qualitatively.

The competition between the two pumping mechanisms, controlled by the relative strengths of W_k^{el} and W_k^{bath} and of W^{mag} and Γ_1 via (9) and (10), is illustrated in Fig. 2. As expected, the reverse Overhauser effect is strongest when $\Gamma_1/W^{\mathrm{mag}} \gg 1$ and $W_k^{\mathrm{el}}/W_k^{\mathrm{bath}} \gg 1$, i.e., when electron spin relaxation and electrically driven spin-flip transitions are strong compared to magnetic ESR driving and hyperfine relaxation, respectively.

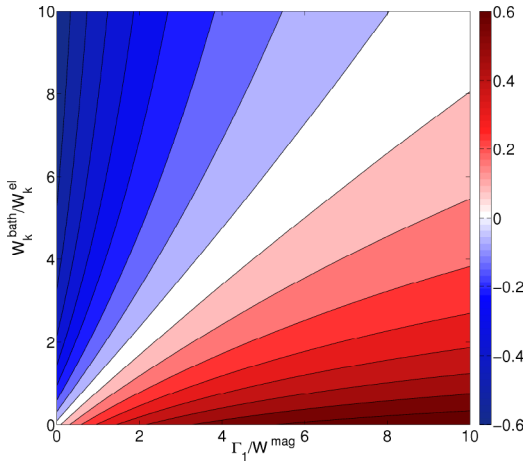

FIG. 2 (color online). Local steady-state nuclear polarization $s_k \equiv N_{k,+} - N_{k,-}$ vs $W_k^{\mathrm{bath}}/W_k^{\mathrm{el}}$ and $\Gamma_1/W^{\mathrm{mag}}$. We obtain s_k from (9) with $\beta\Delta\varepsilon = 2$ (e.g., $B_0 = 750$ mT and $T = 100$ mK) and $\gamma = 0$. Reverse Overhauser pumping dominates below the main diagonal. Because of the spatial dependence of $W_k^{\mathrm{bath}}/W_k^{\mathrm{el}}$, polarizations in different regions of the dot are described by different points in this diagram (see Figs. 1 and 3).

So far we have considered the local polarization described by Eq. (9) and Fig. 2. These results can be directly applied to the entire system in the limit where the homogenization of nuclear polarization takes place on a time scale much shorter than the time scale for polarization buildup. Because this process can be slow [4], we must consider the full spatial dependence of polarization.

To understand the DNP steady states, it is necessary to account for the resonant character of the rates (3) and (8), which are sensitive to the total polarization s due to the hyperfine shift that brings the system into or out of resonance. To this end, we determine the steady-state values of polarization self-consistently by combining expressions (9) and (10) with the definition of s, Eq. (4). This gives a self-consistency condition of the form $s = f(s)$, where the function $f(s)$ is peaked near the value of s where the Overhauser shift brings the electron Zeeman energy into resonance with the driving field. Depending on parameter values, one or more solutions may exist.

The stable and unstable polarization fixed points are plotted in Fig. 1 as a function of driving frequency for parameters deep in the Overhauser and reverse Overhauser regimes with $B_0 = 2$ T, $\Gamma_1 = \Gamma_2 = 10^8$ s^{-1}, and $\gamma = 0.05$ s^{-1}. In the Overhauser regime we use $B_1 = 5$ mT and $W^{\mathrm{bath}} = 5$ s^{-1}, while in the reverse Overhauser regime we use $B_1 = 1$ mT and $d_\omega = 1$ nm. These parameter values were chosen, in a realistic range [2,3,6,19], to clearly exhibit the behavior in the two pumping regimes. When comparing the values of $\Gamma_{1,2}$ with those expected in quantum dots, the reader should bear in mind that these rates are highly sensitive to coupling to the leads [20] and driving strength.

In the Overhauser regime, DNP is in the direction that adds to the external field, leading to ''resonance dragging''

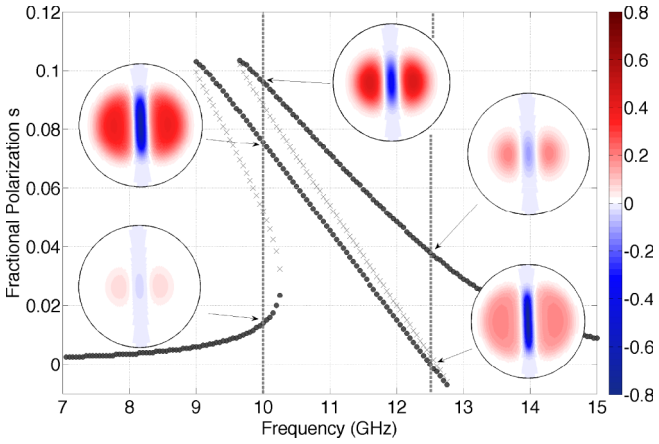

FIG. 3 (color online). Stability diagram in the crossover regime with $B_0 = 2$ T, $B_1 = 2.5$ mT, $d_\omega = 1$ nm, $\Gamma_1 = \Gamma_2 = 10^8$ s^{-1}, $W^{\text{bath}} = 1$ s^{-1}, $\gamma = 0.005$ s^{-1}. Insets show nuclear polarization distributions in the stable states indicated by the arrows. ESR frequency dragging occurs in both sweep directions. The effect is asymmetrical, with maximum shift of 300 MHz in the positive direction and 3.5 GHz in the negative direction.

as frequency is swept from low to high. In the reverse Overhauser regime, DNP is in the opposite direction and the system remains on resonance on the sweep from high to low frequencies. Analogous hysteretic behavior occurs when sweeping magnetic field.

Spatial dependence of polarization arises due to the spatial variations of the rates $W_k^{\text{bath}} \propto |\psi(r_k)|^4$ and $W_k^{\text{el}} \propto |\nabla_x|\psi(r_k)|^2|^2$, where without loss of generality we have taken the external driving $\mathbf{E}(t) \parallel \hat{x}$. Once the steady-state values of the net polarization s are identified, the local nuclear polarization at each point r_k can be found by substituting s into Eq. (9). The resulting polarization distributions $s(r_k) = N_{k,+} - N_{k,-}$, obtained for $|\psi(r)|^2 \propto e^{-r^2/r_0^2}$, are displayed in the insets of Fig. 1.

Because of the dependence $W_k^{\text{el}} \propto |\nabla|\psi(r)|^2|^2$, nuclei on the shoulders of $|\psi(r)|^2$ are most strongly affected by the reverse Overhauser mechanism, while nuclei near the center of the dot are not affected at all. Thus polarization builds up in lobes as in Fig. 1(b) for a linearly polarized driving field, while for a circularly polarized driving field it would build up in a ring. Conversely, nuclear spins near the center of the dot where $|\psi(r)|^2$ is maximal are most strongly pumped by the Overhauser mechanism [Fig. 1(a)].

A more complex behavior is featured by the crossover regime where both mechanisms are of comparable strength. In this case there are additional stable states of DNP, organized as shown in Fig. 3. The corresponding spatial distributions are indicated by the arrows. While the net polarization remains not too large, the system exhibits separate regions of very large positive and negative polarization. Interestingly, resonance dragging can occur in *both* frequency sweep directions in this regime.

The clearest experimental evidence in favor of the proposed mechanism could be obtained, as suggested by Fig. 2, by independently varying the electron spin decay rates Γ_1 and W^{bath} and the ESR excitation strengths W^{mag} and W^{el} in order to observe DNP reversal. Although the process controlling spin relaxation is uncertain, it likely involves cotunneling [11,20]. This would make both Γ_1 and W^{bath} sensitive to the strength of coupling to the leads, which can be adjusted *in situ*. The spatial profile of polarization can also be probed via the dependence of electron Zeeman energy on applied dc electric field. Such a field shifts the electron wave function relative to the DNP, leading to a change in the Overhauser shift [see Eqs. (1) and (4)].

Besides offering an explanation of the anomalous sign of polarization [3], the proposed mechanism of nuclear pumping by electrically driven ESR provides a new tool for controlling nuclear spins. Combined with conventional Overhauser pumping, it can be used to create polarized nuclear states of either sign with spatial modulation on a scale less than the electron confinement radius

We benefited from useful discussions with C. Barthel, D. G. Cory, J. Danon, F. H. L. Koppens, E. A. Laird, C. M. Marcus, Yu. V. Nazarov, E. I. Rashba, and L. M. K. Vandersypen, and partial support from W. M. Keck Foundation Center for Extreme Quantum Information Theory. The work of M. R. work was supported by DOE CSGF, Grant No. DE-FG02-97ER25308.

[1] J. R. Petta *et al.*, Science **309**, 2180 (2005).
[2] F. H. L. Koppens *et al.*, Nature (London) **442**, 766 (2006).
[3] E. A. Laird *et al.*, preceding Letter, Phys. Rev. Lett. **99**, 246601 (2007).
[4] A. V. Khaetskii, D. Loss, and L. Glazman, Phys. Rev. Lett. **88**, 186802 (2002); Phys. Rev. B **67**, 195329 (2003).
[5] W. A. Coish and D. Loss, Phys. Rev. B **72**, 125337 (2005).
[6] A. Imamoglu, E. Knill, L. Tian, and P. Zoller, Phys. Rev. Lett. **91**, 017402 (2003).
[7] D. Stepanenko, G. Burkard, G. Giedke, and A. Imamoglu, Phys. Rev. Lett. **96**, 136401 (2006).
[8] K. Ono and S. Tarucha, Phys. Rev. Lett. **92**, 256803 (2004).
[9] F. H. L. Koppens *et al.*, Science **309**, 1346 (2005).
[10] J. Baugh, Y. Kitamura, K. Ono, and S. Tarucha, Phys. Rev. Lett. **99**, 096804 (2007).
[11] F. H. L. Koppens and L. M. K. Vandersypen (unpublished).
[12] A. Overhauser, Phys. Rev. **92**, 411 (1953).
[13] A. Abragam, Phys. Rev. **98**, 1729 (1955).
[14] *Optical Orientation*, edited by F. Meier and B. P. Zakharchenya (Elsevier Science, Amsterdam, 1984).
[15] D. Gammon *et al.*, Phys. Rev. Lett. **86**, 5176 (2001).
[16] L. H. Bennet and H. C. Torrey, Phys. Rev. **108**, 499 (1957).
[17] W. Yao, R-B. Liu, and L. J. Sham, Phys. Rev. B **74**, 195301 (2006).
[18] J. Danon and Yu. V. Nazarov (private communication).
[19] S. I. Erlingsson and Yu. V. Nazarov, Phys. Rev. B **66**, 155327 (2002).
[20] J. Dreiser *et al.*, arXiv:0705.3557.